nature structural & molecular biology

ARTICLES

https://doi.org/10.1038/s41594-020-0417-5

Allosteric regulation of mammalian Na^+/I^- symporter activity by perchlorate

Alejandro Llorente-Esteban[1,2,5], Rían W. Manville[3], Andrea Reyna-Neyra[1,2,5], Geoffrey W. Abbott[3], L. Mario Amzel[4] ✉ and Nancy Carrasco[1,2,5] ✉

The Na^+/I^- symporter (NIS), the plasma membrane protein that actively transports I^- (stoichiometry $2Na^+$:$1I^-$) in thyroid physiology and radioiodide-based thyroid cancer treatment, also transports the environmental pollutant perchlorate (stoichiometry $1Na^+$:$1ClO_4^-$), which competes with I^- for transport. Until now, the mechanism by which NIS transports different anion substrates with different stoichiometries has remained unelucidated. We carried out transport measurements and analyzed these using a statistical thermodynamics–based equation and electrophysiological experiments to show that the different stoichiometry of ClO_4^- transport is due to ClO_4^- binding to a high-affinity non-transport allosteric site that prevents Na^+ from binding to one of its two sites. Furthermore, low concentrations of ClO_4^- inhibit I^- transport not only by competition but also, critically, by changing the stoichiometry of I^- transport to 1:1, which greatly reduces the driving force. The data reveal that ClO_4^- pollution in drinking water is more dangerous than previously thought.

NIS, encoded by the *SLC5A5* gene, is the key plasma membrane protein that mediates active I^- uptake in the thyroid gland, the first step in the biosynthesis of the thyroid hormones, of which iodine is an essential constituent[1]. Thyroid hormones are critical during embryonic and postembryonic development and for cellular metabolism at all stages of life. The molecular characterization of NIS began in 1996 with our isolation of the complementary DNA that encodes NIS[2]. NIS couples the 'uphill' inward transport of I^- against its electrochemical gradient to the 'downhill' inward translocation of Na^+ down its electrochemical gradient, generated by the Na^+/K^+ ATPase[1,3]. NIS is key in thyroid physiology and has been at the center of radioiodide treatment of thyroid cancer since the 1940s (ref. [4]). One of our first fundamental mechanistic discoveries was that NIS mediates I^- transport with a $2Na^+$:$1I^-$ stoichiometry[5]. One long-standing puzzle about transport by NIS is that the protein accumulates I^- from serum concentrations that are orders of magnitude below the K_M of NIS for I^-. We have shown that there is a simple explanation for this necessary but unusual property: at physiological Na^+ concentrations, 79% of all NIS molecules have two Na^+ ions bound to them, and are therefore poised to bind and transport I^-. As a result, even when very few NIS molecules bind I^-, every bound I^- is transported[6]. Therefore, the mechanism of I^- transport by NIS seems to be an evolutionary adaptation to the scant amount of I^- in the environment[7].

We have demonstrated that the binding of Na^+ to one of the Na^+ sites on NIS significantly increases the affinity of the other Na^+ site for Na^+ (ref. [6]). We have also shown, by scintillation proximity assays using direct $^{22}Na^+$ binding experiments, that there is strong cooperativity between the two Na^+ sites, and that the cooperativity between the two Na^+ sites is lost when residues S353 and T354—Na^+ ligands at the Na2 site—are replaced with alanine[8], even though two Na^+ sites remain present. Therefore, given that allosteric interactions require the protein to have access to multiple conformations, we inferred that other residues besides S353 and T354 participate in the coordination of Na^+ at the Na2 site, a conclusion that was validated when we subsequently determined that residues S66, D191, Q194, and Q263 also participate in Na^+ coordination at the Na2 site[9].

Unlike Cl^- channels and transporters, which transport both Cl^- and I^- (with affinities in the mM range)[10–12], NIS discriminates between these two anions in a remarkable way: it does not transport Cl^-, an anion that is present at concentrations of ~100 mM in the extracellular fluid, but it does transport I^-, which is present at submicromolar concentrations. NIS also translocates a variety of imaging substrates that can be detected by PET (positron emission tomography) ($^{124}I^-$ and $^{18}F\text{-}BF_4^-$) and SPECT-CT (single-photon emission computed tomography) ($^{123}I^-$, $^{125}I^-$, $^{131}I^-$, pertechnetate ($^{99m}TcO_4^-$), and perrhenate ($^{186}ReO_4^-$, $^{188}ReO_4^-$)). Given that NIS actively transports its substrates into the cell, it offers higher detection sensitivity than proteins that only bind their ligands stoichiometrically. As a result, NIS is becoming the counterpart of green fluorescent protein (GFP) or luciferase for imaging studies in humans[13,14].

Other anions that are transported by NIS include thiocyanate (SCN^-), nitrate (NO_3^-), tetrafluoroborate (BF_4^-), hexafluorophosphate (PF_6^-)[5,15–17] and, crucially, the environmental pollutant perchlorate (ClO_4^-). As ClO_4^- is actively transported by NIS, rather than merely acting as a blocker[18]; this strongly suggests that the adverse health effects of ClO_4^- contamination of drinking water are more serious than previously thought, especially for the most vulnerable populations, which include pregnant and nursing women, fetuses, and nursing infants[18–20].

We previously carried out numerous measurements of NIS-mediated transport of I^- and oxyanions, and analyzed the data using a statistical thermodynamics-based formalism that, through global fitting, provided a platform for estimating all of the necessary constants and for identifying the molecular species most

[1]Department of Cellular and Molecular Physiology, Yale School of Medicine, New Haven, CT, USA. [2]Department of Molecular Physiology and Biophysics, Vanderbilt University, Nashville, TN, USA. [3]Bioelectricity Laboratory, Department of Physiology and Biophysics, School of Medicine, University of California, Irvine, CA, USA. [4]Department of Biophysics and Biophysical Chemistry, Johns Hopkins University School of Medicine, Baltimore, MD, USA. [5]Present address: Department of Molecular Physiology and Biophysics, Vanderbilt University, Nashville, TN, USA. ✉e-mail: mamzel@jhmi.edu; nancy.carrasco@vanderbilt.edu

relevant for transport[6]. Here, we present extensive experimental data, analyzed with the same statistical thermodynamics formalism, but including an allosteric site. Remarkably, the mere addition of this one site in one of its two states (occupied or unoccupied) to the existing model reveals the mechanism by which oxyanions change the transport stoichiometry not only for themselves but also, surprisingly, for I^-. This has important physiological consequences: when the $2Na^+$:$1I^-$ electrogenic stoichiometry becomes electroneutral ($1Na^+$:$1I^-$), it decreases the driving force for I^- transport, lowers I^- accumulation, and imperils biosynthesis of the thyroid hormones. Our results strongly suggest that ClO_4^- pollution in drinking water is more dangerous than previously thought[18].

Results

Theoretical background. NIS has an unusual property for a transporter: it transports different anions with different stoichiometries. Although it translocates its physiological substrate, I^-, using two Na^+ ions per I^- transported (Fig. 1a(i)), NIS actively transports other substrates (such as ReO_4^- and ClO_4^-) with a $1Na^+$:1 anion stoichiometry[5,6,18,21]. The mechanism by which NIS transports different anions with different stoichiometries has not yet been elucidated. Thus, on the basis of the statistical thermodynamics formalism and our previous understanding of the NIS transport mechanism, we proposed several hypotheses that could account for the different stoichiometries: (1) binding of the larger oxyanions to their transport (T) site inhibits Na^+ from binding to the NaA site (Fig. 1a(ii)); (2) in addition to their T site, the oxyanions bind to a non-transport (NT) site that partially overlaps with the NaA site (Fig. 1a(iii)); and (3) in addition to their T site, the oxyanions bind to an NT site that allosterically inhibits the binding of Na^+ to the NaA site (Fig. 1a(iv)). In the physiological 2:1 transport, only the species with all three sites occupied can transition from outwardly to inwardly open. Whichever of these three hypotheses is correct, a NIS species in the outward facing conformation with an anion at the T site and only one Na^+ bound must be able to transition to the inward facing conformation, as long as the NT site is occupied. We show here that hypothesis 3 is correct. Strikingly, occupation of the NT site changes not only the stoichiometry of oxyanion transport but also that of I^- transport.

If the difference in stoichiometry between I^- and oxyanion transport by NIS reflects the existence of a high-affinity NT site for the oxyanions (referred to as oX2 when occupied) that either directly or allosterically inhibits the binding of Na^+ to the NaA site (Fig. 1a(iii),1a(iv))[6], the total number of binding sites in NIS is at least four: the anion T site (referred to as I^- when occupied by I^- and as oX1 when occupied by an oxyanion), the two Na^+ sites (NaA and NaB), and the oxyanion NT (oX2) site. Crucially, if so, only the oxyanions have a high affinity for the NT site; the affinity of I^- for this site is extremely low. Furthermore, when the NT site is occupied by an oxyanion, Na^+ cannot bind to the NaA site. Under these assumptions, the species that are able to bind ions from the extracellular fluid, which are named according to the sites within them that are occupied, are as follows (see also Table 1):

In the NIS column, Empty indicates no ions; NaA, NaB, I^-, oX1, and oX2 have one ion; NaA-NaB, NaA-I^-, NaA-oX1, NaB-I^-, NaB-oX1, NaB-oX2, oX2-I^-, and oX1-oX2 have two ions; and NaA-NaB-I^-, NaA-NaB-oX1, NaB-oX2-I^-, and NaB-oX1-oX2 (competent transport species) have three ions.

States contributing to transport. Note that there are no species with I^- at the NT site or with Na^+ at the NaA site when an oxyanion is bound to the NT (oX2) site. The species listed are necessary and sufficient to account for all of the conditions investigated experimentally. The statistical weights ξ of the different species are shown in Table 1, which includes, for completeness, the species with a zero statistical weight. Note also that, as expected, the statistical weights are a function of the ion concentrations. Given that the conformational change required for the transport process is slow ($36 \cdot sec^{-1}$)[5] or much less frequent than the binding and unbinding of ions, NIS can be considered in equilibrium with the extracellular ions, and the fractions of the different species as a function of the concentrations of Na^+ and of the anion(s) can be obtained from the equations derived using the statistical thermodynamics formalism (see Methods) by means of the constants shown in Table 2. In brief, the partition function Z is obtained as the sum of all statistical weights ($Z = \Sigma\xi_{\text{all species}}$), and the rate of transport ν is proportional to the sum of the statistical weights of the species that can carry out transport under the specified experimental conditions divided by the partition function (equation (1)):

$$\nu = \nu_{\max} \cdot \left(\sum \xi_{\text{species that can transport } I^-}\right)/Z \qquad (1)$$

detailed equations are presented in the Methods section, and can be obtained by replacing the ξ_s in equation (1) with the corresponding explicit expressions in Table 1.

When a competent anion is bound to the NT site, Na^+ cannot bind to the NaA site, but NIS can transport an anion (I^- or an oxyanion) at the T site electroneutrally (1:1), driven by transport of one Na^+ at the NaB site. Therefore, two of the species with ions bound to them can transport their bound anion: the species with two Na^+ ions and one anion bound to them, and the species with one Na^+ at the NaB site, an anion at the NT site, and the same or a different anion at the T site. In the case of carrier-free $^{125}I^-$ transport, the population of NIS molecules with I^- bound to them is negligible. Nevertheless, it can be assumed that the rate of transport is proportional to the sum of the fractions of species that are primed to bind I^- and transport it, that is, the species with two Na^+ ions bound to them and the species with an oxyanion at the NT site and a Na^+ at the NaB site.

Estimation of the binding and interaction constants. The model based on the statistical thermodynamics formalism requires the estimation of a number of constants. They include those for the binding of each ion to its binding sites in empty NIS ($K_{a,X} = 1/K_{d,X}$), and the constants that reflect the increase in affinity at one site (y) when another site (x) is occupied ($\phi_{X,Y}$)[6]. The constants can be obtained by fitting the experimental transport data under a large number of conditions (Fig. 1b and Extended Data Fig. 1). The number of constants, however, is too large, and pairs of constants may be correlated for the data to be fitted by (for example) least-squares refinement adjusting all the parameters simultaneously. Fortunately, some of the constants, such as the affinity of empty NIS for the Na^+ ions and I^- and the constants of interaction among these bound ions, as well as the number of binding sites for these ions, have already been obtained by fitting transport data from previous experiments using our statistical thermodynamics formalism and by direct Na^+ binding experiments[6,8]. Using these values, the new constants were obtained by a combination of least-squares refinement of small groups of parameters and manual fitting. The improvement in the value of χ^2 was used to monitor the progress of the refinement. The values of the constants are shown in Table 2. In comparing the previously reported values for the K_ds of ClO_4^- and ReO_4^- for the T site with the values in Table 2, it must be noted that the estimation of the previous values did not take into account the binding of the oxyanions to the NT site. As the K_d values for the NT site are lower than those for the T site, the previous values represent binding to the T site when the NT site is mostly occupied. Given that binding to the NT site increases the affinity of the oxyanion for the T site by $\varphi_{oX1,oX2}$, the affinities equivalent to those obtained in previous experiments are K_d (previously reported) $\approx K_d$ (Table 2)/$\phi_{oX1,oX2}$.

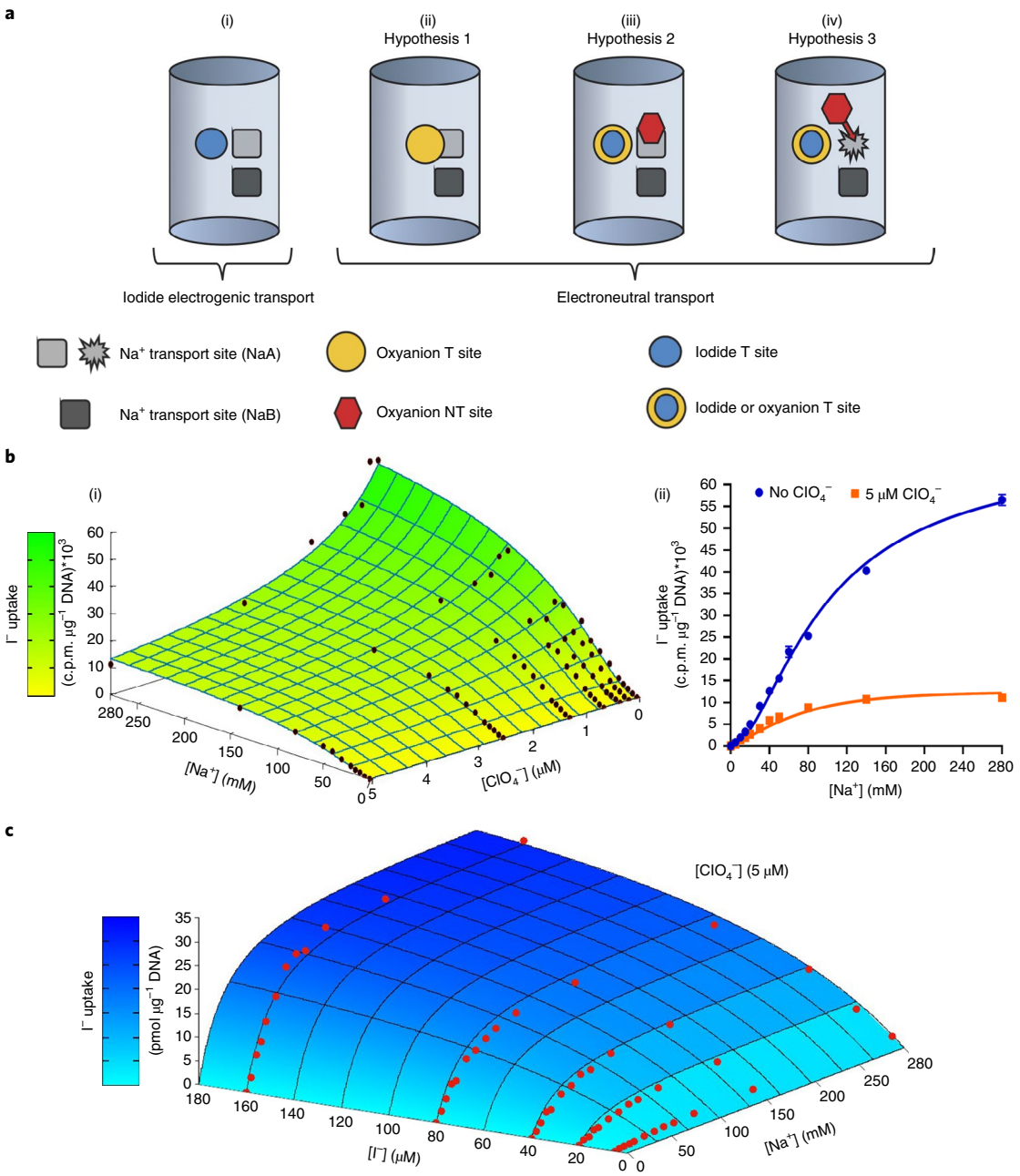

Fig. 1 | ClO_4^- changes the mechanism of NIS-mediated I^- transport. a, Possible hypotheses for how NIS transports different substrates with different stoichiometries. (**i**), Electrogenic transport: $2Na^+$ ions and I^- are translocated. (**ii**–**iv**), Hypotheses for electroneutral transport: (**ii**) Hypothesis 1: one Na^+ ion and one oxyanion are translocated. Oxyanion transport (T) site (yellow circle) partially overlaps with the NaA site (light gray square), thus inhibiting binding of Na^+ to this site; I^- is not transported electroneutrally because its binding to its T site (blue circle) does not partially overlap with the NaA site. (**iii**) Hypothesis 2: oxyanion non-transport (NT) site (red hexagon) partially overlaps with the NaA site (light gray square), thus inhibiting binding of Na^+ to this site; high concentrations of Na^+ outcompete the oxyanion at the NT site (red hexagon) and restore electrogenic transport of I^-. (**iv**) Hypothesis 3: binding of the oxyanion to an NT site (red hexagon) allosterically inhibits binding of one Na^+ to the NaA site (light gray square) (no overlap); I^- is transported electroneutrally in the presence of an oxyanion. **b**, ClO_4^-changes the stoichiometry of NIS-mediated I^- transport. Initial rates (4-min time points) of I^- transport at different concentrations of Na^+ and ClO_4^- (0–5 µM); carrier-free $^{125}I^-$ was used as a tracer. (**i**) Points represent the mean of duplicate or triplicate $^{125}I^-$ uptake data. The surface, calculated with equation (3A), represents the rate of transport, expressed as the fraction of NIS molecules that are occupied by $2Na^+$ ions and the fraction occupied by $1Na^+$ and ClO_4^- at the NT site. (**ii**) Data from panel (**i**), showing only the experimental points at 0 µM and 5 µM ClO_4^-. **c**, The change in the stoichiometry of I^- transport from electrogenic to electroneutral brought about by ClO_4^- persists even at high concentrations of I^-. Initial rates (4-min time points) of I^- transport at different concentrations of I^-, at a constant concentration of ClO_4^- (5 µM), and as a function of the Na^+ concentration. The surface was calculated using equation (3B). Points represent the mean of duplicate or triplicate $^{125}I^-$ uptake experiments. Data for graphs in **b**,**c** are available as source data.

Using the values in Table 2, $K_{d,ClO_4^-} = 8.93/3.70 = 2.41$ µM and $K_{d,ReO_4^-} = 2.01/2.29 = 0.88$ µM—values highly similar to those reported previously (1.5 and 2.3 µM, respectively)[5].

Low concentrations of an oxyanion (ClO_4^- or ReO_4^-) change the stoichiometry of NIS-mediated I^- transport from electrogenic to electroneutral. To decide among our hypotheses (Fig. 1a),

transport kinetics of carrier-free $^{125}I^-$ were measured as a function of the Na^+ concentration for different concentrations of ClO_4^- (Fig. 1b) or ReO_4^- (Extended Data Fig. 1). In the absence of any oxyanion, the dependence of I^- transport on the Na^+ concentration was clearly sigmoidal, as would be expected given the $2Na^+$:$1I^-$ stoichiometry of NIS-mediated I^- transport. As the concentration of ClO_4^- or ReO_4^- was increased from 0 to 5 µM, three effects were observed: (1) the dependence of I^- transport on the Na^+ concentration became progressively less sigmoidal, eventually switching to hyperbolic (that is, indicating a shift toward an electroneutral 1 Na^+:1 I^- stoichiometry), likely owing to binding of the oxyanion to the proposed NT site; (2) the apparent affinity for Na^+ increased (K_M 134.6 ± 12.5 mM in the absence of ClO_4^- and 43.5 ± 1.9 mM at 5 µM ClO_4^-), which is an expected effect because the binding of one of the substrates increases the affinity of NIS for the other substrate[6,8]; (3) at the higher oxyanion concentrations, I^- transport was also inhibited by competition between the oxyanion and I^- for binding to the T site, and this was reflected in a decrease in the v_{max}. These observations are exactly in line with the existence of an allosteric NT site that, when occupied by an oxyanion, inhibits Na^+ from binding to the NaA site (Fig. 1a(iv)). The affinities of the NT site for ClO_4^- and ReO_4^-, estimated using the general statistical thermodynamics-based equation (1), are 1.6 µM and 0.79 µM, respectively (Table 2).

Moreover, if hypothesis 1 were correct (Fig. 1a(ii)), not only would high I^- concentrations outcompete the oxyanion at the anion T site but high concentrations of Na^+ would also outcompete the oxyanion because of the proposed overlap between the T and NaA sites. Thus, high concentrations of either I^- or Na^+ would result in electrogenic I^- transport even in the presence of an oxyanion; in fact, neither of these outcomes was observed in our results. Instead, kinetic experiments carried out at different Na^+ and I^- concentrations in the presence of 5 µM ClO_4^- (Fig. 1c) or 5 µM ReO_4^- (Extended Data Fig. 2) showed that the dependence of I^- transport on the Na^+ concentration remains hyperbolic (that is, transport is electroneutral with a $1Na^+$: $1I^-$ stoichiometry) for I^- concentrations as high as 160 µM or Na^+ concentrations as high as 280 mM, clearly ruling out hypothesis 1. Furthermore, high concentrations of Na^+ did not have an effect on the v_{max} of ReO_4^- transport[6], which is consistent with this conclusion.

Similarly, if hypothesis 2 (Fig. 1a(iii)) were correct (that is, if the NaA site and an NT site partially overlapped), high concentrations of Na^+ would displace the oxyanion from the NT site and render I^- transport electrogenic—which, as mentioned, did not occur even at 280 mM (Fig. 1c), ruling out hypothesis 2 as well. However, I^- transport remained electroneutral even at high concentrations of Na^+, which is consistent with the idea that the oxyanion binds to the NT site and causes it to allosterically inhibit the binding of Na^+ to the NaA site, as proposed in hypothesis 3 (Fig. 1a(iv)). In summary, low concentrations of an oxyanion (<5 µM) change the stoichiometry of NIS-mediated I^- transport from electrogenic to electroneutral in wild-type (WT) NIS. In addition, I^- does not bind to the NT oX2 site.

Oxyanions markedly decrease the K_M of WT NIS for I^-, but have no effect on the K_M of G93T NIS for I^-. We have reported previously that, in contrast to WT NIS, the G93T NIS mutant transports ClO_4^- and ReO_4^- electrogenically, even at an oxyanion concentration of 1 mM (refs. [5,21]) (a concentration 200 times that required to saturate the NT site), indicating that when Gly 93 is replaced with Thr, the mechanism of NIS undergoes a dramatic change, such that the oxyanion does not inhibit Na^+ binding to the NaA site[6]. We have also reported that the K_M of G93T NIS for I^- is higher (K_M = 303.8 ± 24.1 µM; that is, a lower apparent affinity for I^-) than that of WT NIS (K_M = 23.12 ± 1.30 µM) (Fig. 2a,b, blue),[21]. We now demonstrate here that ClO_4^- (5 µM) decreased the v_{max} of I^- transport mediated by WT and G93T NIS (Fig. 2a,b, orange), because ClO_4^- binds to the T site in both. In contrast, whereas ClO_4^- (5 µM) had virtually no effect on the K_M of G93T NIS for I^- (K_M = 307.7 ± 34.5 µM) (Fig. 2b, orange), it did increase the K_M of WT NIS for I^- as much as sixfold (K_M = 137.9 ± 18.9 µM) (Fig. 2a, orange). This is because ClO_4^- switches the Na^+:I^- stoichiometry

Table 1 | Species present in the experiments and their statistical weights (ξ)

NIS species	Statistical weight (ξ)
Empty	1
NaA	$K_{NA} \cdot [Na^+]$
NaB	$K_{NB} \cdot [Na^+]$
oX1	$K_{oX1} \cdot [XO_4^-]$
[a]I^-	$K_{I^-} \cdot [I^-]$
oX2	$K_{oX2} \cdot [XO_4^-]$
NaA·NaB	$K_{NA} \cdot K_{NB} \cdot \phi_{NA,NB} \cdot [Na^+]^2$
oX1·oX2	$K_{oX1} \cdot K_{oX2} \cdot \phi_{oX1,oX2} \cdot [XO_4^-]^2$
[a]I^-·oX2	$K_{I^-} \cdot K_{oX2} \cdot \phi_{I^-,oX2} \cdot [XO_4^-] \cdot [I^-]$
[b]NaA·oX2	0
NaA·oX1	$K_{NA} \cdot K_{oX1} \cdot \phi_{NA,oX1} \cdot [Na^+] \cdot [XO_4^-]$
[a]NaA·I^-	$K_{NA} \cdot K_{I^-} \cdot \phi_{NA,I^-} \cdot [Na^+] \cdot [I^-]$
NaB·oX1	$K_{NB} \cdot K_{oX1} \cdot \phi_{NB,oX1} \cdot [Na^+] \cdot [XO_4^-]$
NaB·oX2	$K_{NB} \cdot K_{oX2} \cdot \phi_{NB,oX2} \cdot [Na^+] \cdot [XO_4^-]$
[a]NaB·I^-	$K_{NB} \cdot K_{I^-} \cdot \phi_{NB,I^-} \cdot [Na^+] \cdot [I^-]$
NaA·NaB·oX1	$K_{NA} \cdot K_{NB} \cdot K_{oX1} \cdot \phi_{NA,NB} \cdot \phi_{NA,oX1} \cdot \phi_{NB,oX1} \cdot [Na^+]^2 \cdot [XO_4^-]$
[a]NaA·NaB·I^-	$K_{NA} \cdot K_{NB} \cdot K_{I^-} \cdot \phi_{NA,NB} \cdot \phi_{NA,I^-} \cdot \phi_{NB,I^-} \cdot [Na^+]^2 \cdot [I^-]$
[b]NaA·oX1·oX2	0
[a,b]NaA· I^-·oX2	0
[b]NaA·NaB·oX2	0
NaB·oX1·oX2	$K_{NB} \cdot K_{oX1} \cdot K_{oX2} \cdot \phi_{NB,oX1} \cdot \phi_{NB,oX2} \cdot \phi_{oX1,oX2} \cdot [Na^+] \cdot [XO_4^-]^2$
[a]NaB·oX2·I^-	$K_{NB} \cdot K_{oX2} \cdot K_{I^-} \cdot \phi_{NB,oX2} \cdot \phi_{NB,I^-} \cdot \phi_{I^-,oX2} [Na^+] \cdot [XO_4^-] \cdot [I^-]$
[b]NaA·NaB·oX1·oX2	0
[a,b]NaA·NaB·I^-·oX2	0

[a]Terms with I^-: I^- does not bind to the allosteric NT site (oX2). [b]Terms with oX2 and NaA occupied (statistical weight = 0).

Table 2 | Global adjustment of the data

	K_d				Φ				
	NaA (mM)	NaB (mM)	oX1 (µM)	oX2 (µM)	NaA,NaB	oX1,oX2	oX2,NaB	oX1,NaA	oX1,NaB
ClO_4^-	138.89 ± 5.6	526.32 ± 13.4	8.93 ± 0.4	1.67 ± 0.5	12.23 ± 0.3	3.70 ± 0.5	3.35 ± 0.3	3.00 ± 0.2	2.50 ± 0.1
ReO_4^-	140.06 ± 4.7	526.32 ± 12.5	2.01 ± 0.1	0.79 ± 0.1	7.38 ± 0.2	2.29 ± 0.3	2.90 ± 0.3	2.93 ± 0.1	2.90 ± 0.1

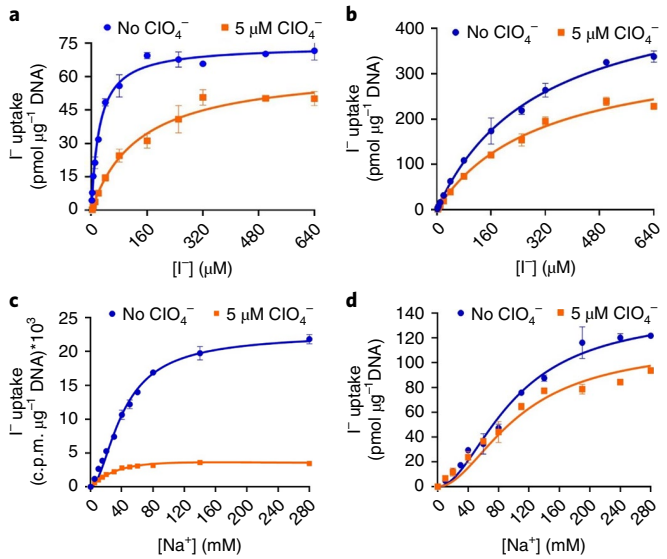

Fig. 2 | Differential effects of ClO_4^- on the transport stoichiometry of WT and G93T NIS and on their K_M values for I^-. a,**b**, Initial rates of I^- transport at different concentrations of I^- (1.25–640 μM) at 140 mM Na^+ in the absence (blue line) or presence (orange line) of ClO_4^- (5 μM) for WT NIS (**a**) and G93T NIS (**b**). **c**,**d**, Initial rates of $^{125}I^-$ transport at different concentrations of Na^+ (0–280 mM) for WT NIS (**c**) using carrier-free $^{125}I^-$ in the absence (blue line) or presence (orange line) of ClO_4^- (5 μM) (data expressed as c.p.m. μg^{-1} DNA) and for G93T NIS (**d**) using 750 μM $^{125}I^-$ (specific activity 35 μCi μmol^{-1}) in the absence (blue line) or presence (orange line) of ClO_4^- (5 μM). Points represent the mean of duplicate or triplicate $^{125}I^-$ uptake experiments, error bars represent s.d. Data are expressed as pmol I^-μg^{-1} DNA. Data for all graphs are available as source data.

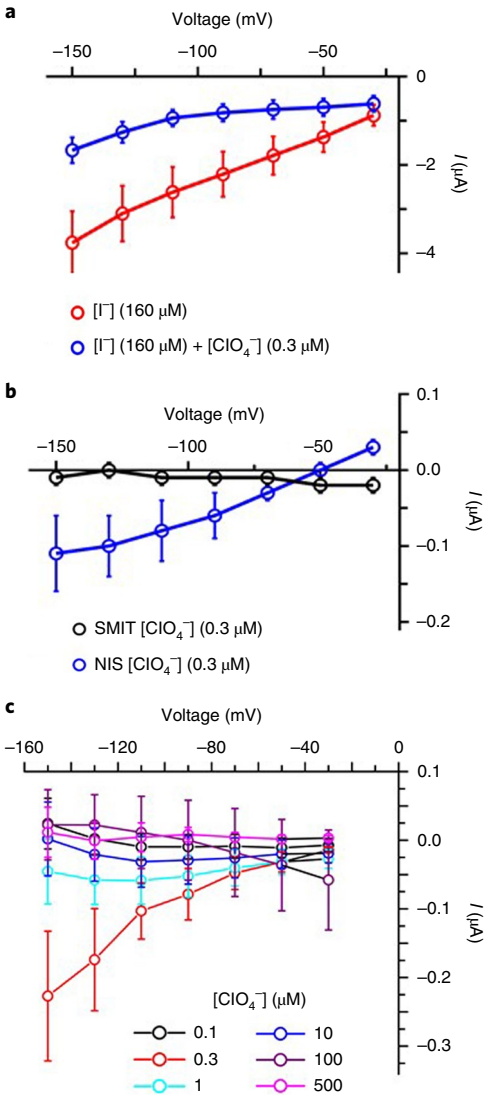

Fig. 3 | ClO_4^- at low concentrations is transported electrogenically by NIS. **a**, Current–voltage relationships recorded by TEVC in oocytes expressing NIS upon addition of I^- (160 μM), in the presence (n = 9) or absence of ClO_4^- (0.3 μM) (n = 7) in bath solution. **b**, Effect of ClO_4^- (0.3 μM) on current–voltage relationships recorded by TEVC in oocytes expressing NIS (n = 10) or SMIT (n = 10). **c**, Current–voltage relationships recorded by TEVC in oocytes expressing NIS with 0.1 (n = 12), 0.3 (n = 5), 1 (n = 10), 10 (n = 9), or 500 (n = 4) μM ClO_4^- in the bath solution. Error bars, s.e.m. Data for all graphs are available as source data.

from 2:1 to 1:1 in WT NIS (Fig. 2c) but not in G93T NIS (Fig. 2d). Taken together, these data strongly suggest that, in G93T NIS, either ClO_4^- cannot bind to the allosteric NT site or, if it does bind to it, the resulting conformational change that would prevent Na^+ from binding to the NaA site is impaired.

ClO_4^- elicits NIS-mediated currents when its concentration is lower than that necessary to saturate the NT site. With respect to ClO_4^-transport by WT NIS, our hypothesis (Fig. 1a(iv)) predicts that at ClO_4^- concentrations lower than the K_d of ClO_4^- for the NT site (1.6 μM, Table 2), ClO_4^- should be transported, at least partially, with an electrogenic $2Na^+$:$1ClO_4^-$ stoichiometry. This is because, under these conditions, the NT site will only be partially occupied by ClO_4^- and some NIS molecules will bind Na^+ to the NaA and NaB sites and ClO_4^- to the T site (Fig. 1a(iv)). To test this key prediction, we carried out electrophysiological experiments in *Xenopus laevis* oocytes heterologously expressing NIS. First, we showed that the addition of I^- (160 μM) to the medium elicited negative currents (indicating positive charges moving into the interior of the oocyte) owing to the $2Na^+$:$1I^-$ stoichiometry of transport[5,21] (Fig. 3a, red). Second, in the presence of only 0.3 μM ClO_4^-, the currents elicited by I^- were substantially reduced (Fig. 3a, blue), suggesting that ClO_4^- had bound to the allosteric NT site without saturating it, and that, as a result, the stoichiometry of I^- transport had become nearly electroneutral. Third, in perhaps the most dramatic validation of hypothesis 3, we showed that the prediction laid out above was correct: ClO_4^- at low concentrations (0.3 μM; that is, lower than the K_d of ClO_4^- for the NT site) actually elicited currents (Fig. 3b, blue), the hallmark of electrogenic transport of ClO_4^-. Our previous reports[5,21] that ClO_4^- did not elicit currents in NIS-expressing *X. laevis* oocytes (albeit at high ClO_4^- concentrations (500 μM)) would make our current finding of electrogenic ClO_4^- transport at low ClO_4^- concentrations all the more unexpected, were it not for our newly proposed hypothesis 3. We demonstrated that these currents were mediated by NIS by showing that no currents were elicited by ClO_4^- when the Na^+-dependent *myo*-inositol transporter (SMIT)[22], another member of the SLC5 family (encoded by *SLC5A3*), was expressed in the oocytes instead of NIS (Fig. 3b, black). It is not surprising that ClO_4^- currents are 40 times smaller than those generated by I^-, because the I^- concentration (160 μM) was more than 500 times the concentration of ClO_4^- (0.3 μM). Moreover, saturating the allosteric NT site by increasing the concentration of ClO_4^- abolished the ClO_4^--induced currents (Fig. 3c), as predicted by hypothesis 3 (Fig. 1a(iv)).

Discussion

In summary, by showing that oxyanions (such as ClO_4^-) at concentrations as low as 5 μM or less change the stoichiometry of WT NIS-mediated I^- transport from electrogenic to electroneutral, we reveal the existence of an NT site that, upon binding an oxyanion, allosterically inhibits the binding of Na^+ to the NaA site. Our experiments were carefully designed to shed light on the regulation of the transport stoichiometry and mechanism of NIS; furthermore, we developed a general statistical thermodynamics-based equation[23] that contains terms representing all species contributing to transport under all conditions, and used it to demonstrate the existence of the NT site. In previous research, we focused on mechanistic aspects of the simplest case of NIS activity: transport of a single anion[6]. Here, we investigated more complex cases of NIS-mediated transport, including oxyanion binding, transport, and changes in Na^+/anion stoichiometry. The omission of a number of species ($\xi = 0$; Table 1)—NIS species with an oxyanion at the NT site and Na^+ at the NaA site, and NIS species with I^- at the NT site (as posited by hypothesis 3)—is key to the success of the model. As described, the model allows the same equation (in its two forms; equation (3A) and equation (3B)) to be used to fit the data from all of the experiments performed. Being able to use a single equation is valuable, as this obviates the need to make experiment-specific assumptions (that is, different and independent v_{max} and K_M values for each curve) in interpreting the results.

Even low concentrations of ClO_4^- radically change the mechanism of NIS-mediated I^- transport, by changing the driving force from $2Na^+$ to $1Na^+$ and increasing the K_M of NIS for I^- sixfold; less transport of I^- will result in a decrease in the biosynthesis of thyroid hormones. This reveals that contamination of drinking water with ClO_4^- is even more dangerous than previously thought, especially for the most vulnerable populations, including pregnant and nursing women and their fetuses and nursing newborns. NIS expressed in the lactating breast mediates active I^- transport into the milk[24]; therefore, if a nursing mother drinks water containing ClO_4^-, not only will there be less I^- in her milk but ClO_4^- will also be actively translocated into the milk. As a result, I^- uptake for thyroid hormone biosynthesis by the newborn will itself be inhibited by ClO_4^-, both because it will compete for the T site and because it will change the Na^+/I^- stoichiometry from 2:1 to 1:1—at precisely those early stages of life when thyroid hormones are essential for the maturation of the central nervous system, lungs, and skeletal system[17]. NIS is also expressed in the placenta[25,26], where it transports I^- from the mother into the fetus' bloodstream—which is crucial, as the fetus synthesizes 70% of its own thyroid hormones. Therefore, if a pregnant woman drinks water contaminated with high concentrations of ClO_4^-, it can gravely harm the developing fetus.

One intriguing question that deserves future investigation is whether or not the allosteric NT site evolved to maintain homeostasis by binding a physiological anion when thyroid hormone levels are high. It will likewise be of great interest to determine whether other transporters have an allosteric NT substrate binding site that regulates their activity similarly to how the NT site modulates NIS function. It is likely that the second substrate binding sites in LeuT, vSGLT, PutP, and MhsT[27–29] are different from the NT allosteric oxyanion site in NIS. Those sites have been proposed to bind leucine, galactose, proline, and hydrophobic amino acids, respectively, and binding of these substrates does not change the stoichiometry of transport (for example, leucine binding by LeuT and leucine transport by MhsT as a function of the Na^+ concentration at saturating concentrations of leucine are still sigmoidal ($2\,Na^+$)[29,30]). By contrast, the allosteric site in NIS does not bind I^-, it only binds the oxyanions, and this oxyanion binding does change the mechanism of transport from electrogenic to electroneutral. If the allosteric site in NIS were similar to the proposed second substrate binding sites in LeuT, vSGLT, PutP, and MhsT, it would bind I^-, and we show that this is not the case.

Finding allosteric regulation of the transport stoichiometry of other membrane transporters by NT binding sites would not only deepen our understanding of these transporters but may also make it possible to eventually develop novel drug targets.

Online content

Any methods, additional references, Nature Research reporting summaries, source data, extended data, supplementary information, acknowledgements, peer review information; details of author contributions and competing interests; and statements of data and code availability are available at https://doi.org/10.1038/s41594-020-0417-5.

Received: 10 August 2019; Accepted: 12 March 2020;
Published online: 25 May 2020

References

1. Carrasco, N. Iodide transport in the thyroid gland. *Biochim. Biophys. Acta* **1154**, 65–82 (1993).
2. Dai, G., Levy, O. & Carrasco, N. Cloning and characterization of the thyroid iodide transporter. *Nature* **379**, 458–460 (1996).
3. De La Vieja, A., Dohan, O., Levy, O. & Carrasco, N. Molecular analysis of the sodium/iodide symporter: impact on thyroid and extrathyroid pathophysiology. *Physiol. Rev.* **80**, 1083–1105 (2000).
4. Seidlin, S. M., Marinelli, L. D. & Oshry, E. Radioactive iodine therapy; effect on functioning metastases of adenocarcinoma of the thyroid. *J. Am. Med. Assoc.* **132**, 838–847 (1946).
5. Eskandari, S. et al. Thyroid Na^+/I^- symporter. Mechanism, stoichiometry, and specificity. *J. Biol. Chem.* **272**, 27230–27238 (1997).
6. Nicola, J. P., Carrasco, N. & Amzel, L. M. Physiological sodium concentrations enhance the iodide affinity of the Na^+/I^- symporter. *Nat. Commun.* **5**, 3948 (2014).
7. Portulano, C., Paroder-Belenitsky, M. & Carrasco, N. The Na^+/I^- symporter (NIS): mechanism and medical impact. *Endocr. Rev.* **35**, 106–149 (2014).
8. Ravera, S., Quick, M., Nicola, J. P., Carrasco, N. & Amzel, L. M. Beyond non-integer Hill coefficients: a novel approach to analyzing binding data, applied to Na^+-driven transporters. *J. Gen. Physiol.* **145**, 555–563 (2015).
9. Ferrandino, G. et al. Na^+ coordination at the Na2 site of the Na^+/I^- symporter. *Proc. Natl Acad. Sci. USA* **113**, E5379–E5388 (2016).
10. Stephens, C. E., Whittamore, J. M. & Hatch, M. ^{125}Iodide as a surrogate tracer for epithelial chloride transport by the mouse large intestine in vitro. *Exp. Physiol.* **104**, 334–344 (2019).
11. Twyffels, L. et al. Anoctamin-1/TMEM16A is the major apical iodide channel of the thyrocyte. *Am. J. Physiol. Cell Physiol.* **307**, C1102–C1112 (2014).
12. Valdez-Flores, M. A. et al. Functionomics of NCC mutations in Gitelman syndrome using a novel mammalian cell-based activity assay. *Am. J. Physiol. Renal Physiol.* **311**, F1159–F1167 (2016).
13. Urnauer, S. et al. EGFR-targeted nonviral NIS gene transfer for bioimaging and therapy of disseminated colon cancer metastases. *Oncotarget* **8**, 92195–92208 (2017).
14. Miller, A. & Russell, S. J. The use of the NIS reporter gene for optimizing oncolytic virotherapy. *Expert Opin. Biol. Ther.* **16**, 15–32 (2016).
15. Jiang, H. et al. Synthesis and evaluation of ^{18}F-hexafluorophosphate as a novel PET probe for imaging of sodium/iodide symporter in a murine C6-glioma tumor model. *Bioorg. Med. Chem.* **26**, 225–231 (2018).
16. Nagarajah, J. et al. Sustained ERK inhibition maximizes responses of BrafV600E thyroid cancers to radioiodine. *J. Clin. Invest.* **126**, 4119–4124 (2016).
17. Ravera, S., Reyna-Neyra, A., Ferrandino, G., Amzel, L. M. & Carrasco, N. The sodium/iodide symporter (NIS): molecular physiology and preclinical and clinical applications. *Annu. Rev. Physiol.* **79**, 261–289 (2017).
18. Dohan, O. et al. The Na^+/I symporter (NIS) mediates electroneutral active transport of the environmental pollutant perchlorate. *Proc. Natl Acad. Sci. USA* **104**, 20250–20255 (2007).
19. Dunn, J. T. & Delange, F. Damaged reproduction: the most important consequence of iodine deficiency. *J. Clin. Endocrinol. Metab.* **86**, 2360–2363 (2001).
20. Morreale de Escobar, G. & Escobar del Rey, F. Iodine during pregnancy, lactation and infancy. Minimum and maximum doses: from micrograms to grams. *An. Esp. Pediatr.* **53**, 1–5 (2000).
21. Paroder-Belenitsky, M. et al. Mechanism of anion selectivity and stoichiometry of the Na^+/I^- symporter (NIS). *Proc. Natl Acad. Sci. USA* **108**, 17933–17938 (2011).
22. Manville, R. W., Neverisky, D. L. & Abbott, G. W. SMIT1 modifies KCNQ channel function and pharmacology by physical interaction with the pore. *Biophys. J.* **113**, 613–626 (2017).

23. Shea, M. A. & Ackers, G. K. The O_R control system of bacteriophage lambda. A physical-chemical model for gene regulation. *J. Mol. Biol.* **181**, 211–230 (1985).
24. Tazebay, U. H. et al. The mammary gland iodide transporter is expressed during lactation and in breast cancer. *Nat. Med.* **6**, 871–878 (2000).
25. Di Cosmo, C. et al. The sodium-iodide symporter expression in placental tissue at different gestational age: an immunohistochemical study. *Clin. Endocrinol.* **65**, 544–548 (2006).
26. Mitchell, A. M. et al. Sodium iodide symporter (NIS) gene expression in human placenta. *Placenta* **22**, 256–258 (2001).
27. Li, Z. et al. Identification of a second substrate-binding site in solute-sodium symporters. *J. Biol. Chem.* **290**, 127–141 (2015).
28. Quick, M. et al. The LeuT-fold neurotransmitter:sodium symporter MhsT has two substrate sites. *Proc. Natl Acad. Sci. USA* **115**, E7924–E7931 (2018).
29. Shi, L., Quick, M., Zhao, Y., Weinstein, H. & Javitch, J. A. The mechanism of a neurotransmitter:sodium symporter – inward release of Na^+ and substrate is triggered by substrate in a second binding site. *Mol. Cell* **30**, 667–677 (2008).
30. Fitzgerald, G. A. et al. Quantifying secondary transport at single-molecule resolution. *Nature* **575**, 528–534 (2019).

Methods

Cell culture. The rat intestinal epithelial cell line IEC-6 was used to study the effects of ClO_4^- in cell lines that endogenously express WT NIS[31]. Madin-Darby canine kidney (MDCK) cells stably expressing WT human NIS or the mutant G93T human NIS were used to study the effect of ClO_4^- on the human protein. IEC-6 and MDCK cells were grown in DMEM supplemented with 10% fetal bovine serum, 100 units ml^{-1} penicillin-streptomycin. All tissue culture reagents were from Life Technologies. All cell lines were grown in a humidified atmosphere with 5% CO_2 at 37 °C. Cell lines were not tested for mycoplasma.

Iodide transport experiments. IEC-6 and MDCK cells were plated on 24-well plates 24 h before the experiment. Kinetic experiments were carried out as reported previously[6,21]. In brief, I^- kinetics were performed using a range of I^- concentrations from 0.75 to 640 µM, at 140 mM Na^+, in the presence or absence of 5 µM ClO_4^-. The specific activity of $^{125}I^-$ was 35 µCi µmol^{-1} (Perkin-Elmer). Na^+-dependent kinetics of $^{125}I^-$ transport were carried out with carrier-free $^{125}I^-$ and a range of Na^+ concentrations from 0 to 280 mM, keeping the osmolarity constant (280 mM) with choline chloride. The oxyanion concentrations used were 0, 0.16, 0.31, 0.62, 1.25, 2.5, and 5 µM. Background, obtained in cells at 0 mM Na^+, was subtracted. Amounts of accumulated I^- (pmol) at 4 min were standardized by the amount of DNA per well.

Global equation for data analysis. In brief, the partition function Z is obtained as the sum of all statistical weights ξ ($Z = \Sigma\xi_{\text{all species}}$) presented in Table 1. The rate of transport v is considered to be proportional to the sum of the statistical weights of the species that can carry out transport under the specified experimental conditions divided by the partition function.

$$\nu = \nu_{max} \cdot \left(\sum \xi_{\text{species that can transport } I^-}\right)/Z \quad (2)$$

For the analysis of the experiments carried out with carrier-free $^{125}I^-$, equation (1) becomes equation (3A):

$$\nu = \nu_{max} \cdot (K_{NA} \cdot K_{NB} \cdot \phi_{NA,NB} \cdot [Na^+]^2 + K_{NB} \cdot K_{oX2} \cdot \phi_{NB,oX2} \cdot [Na^+] \cdot [XO_4^-])/Z \quad (3A)$$

For the analysis of the experiments carried out as a function of $[I^-]$, equation (1) becomes equation (3B):

$$\nu = \nu_{max} \cdot \left(K_{NA} \cdot K_{NB} \cdot K_{I^-} \cdot \phi_{NA,NB} \cdot \phi_{NA,I^-} \cdot \phi_{NB,I^-} \cdot [Na^+]^2 \cdot [I^-] + K_{NB} \cdot K_{oX2} \cdot K_{I^-} \cdot \phi_{NB,oX2} \cdot \phi_{NB,I^-} \cdot \phi_{I^-,oX2} \cdot [Na^+] \cdot [XO_4^-] \cdot [I^-]\right)/Z \quad (3B)$$

Determination of the constants. 456 experimental data points were analyzed through global adjustment of the data. Each curve presented in the figures shows the average of duplicates or triplicates for each point value corresponding to each concentration. I^- transport data were fitted using equation (3A) for four groups in the $^{125}I^-$ carrier-free experiments (0 and 5 µM ClO_4^- and 0 and 5 µM ReO_4^-). I^- transport, as a function of the I^- concentration data, was fitted using equation (3B) for two groups of the experiments (5 µM ClO_4^- and 5 µM ReO_4^- (the data for 0 µM oxyanions have been published))[6]. Refinement of the parameters to optimize the fit of the data to equation (3A) or equation (3B) was carried out through least squares[32] and manual adjustment with the program Gnuplot 5.0 Patchlevel 7.

cRNA preparation and *X. laevis* oocyte injection. cRNA transcripts encoding human NIS and SMIT1 were generated by in vitro transcription using the T7 polymerase mMessage mMachine kit (Thermo Fisher Scientific), after vector linearization. cRNA was quantitated by spectrophotometry. Defolliculated stage V and VI *X. laevis* oocytes (Ecocyte Bioscience) were injected with NIS or SMIT1 cRNA (10–20 ng). The oocytes were incubated at 16 °C in Barth's saline solution (Ecocyte) containing penicillin and streptomycin, with daily washing, for 5 d prior to two-electrode voltage-clamp (TEVC) recording.

Two-electrode voltage clamp. TEVC was performed at room temperature (20–22 °C) using an OC-725C amplifier (Warner Instruments) and pClamp10 software (Molecular Devices) 5 d after cRNA injection as described in the section above. For recording, the oocytes were placed in a small-volume oocyte bath (Warner) and were viewed with a dissection microscope. Chemicals were from Sigma. Bath solution was (in mM): 96 NaCl, 4 KCl, 1 $MgCl_2$, 1 $CaCl_2$, 10 HEPES (pH 7.6). ClO_4^- and I^- were stored as 1 M stocks and diluted to working concentrations each experimental day. The anions were introduced into the oocyte recording bath by gravity perfusion at a constant flow of 1 ml min^{-1} for 3 min prior to recording. Pipettes were of 1–2 MΩ resistance when filled with 3 M KCl. Currents were recorded in response to pulses between −150 mV and −10 mV at 20-mV intervals, from a holding potential of −50 mV, to yield current–voltage relationships. Electrophysiology data analysis was performed with Clampfit (Molecular Devices) and Graphpad Prism software (GraphPad); values are stated as means ± s.e.m.

Reporting Summary. Further information on research design is available in the Nature Research Reporting Summary linked to this article.

Data availability

The source data for Figs. 1b,c,2,3, and Extended Data Figs. 1,2 are available in the online version of the paper.

References

31. Nicola, J. P. et al. The Na^+/I^- symporter mediates active iodide uptake in the intestine. *Am. J. Physiol. Cell. Physiol.* **296**, C654–C662 (2009).
32. Marquardt, D. W. An algorithm for least-squares estimation of nonlinear parameters. *J. Soc. Indust. Appl. Math.* **11**, 431–441 (1963).

Acknowledgements

We thank H. Wade and A. Lau and the members of the Carrasco laboratory for critical reading of the manuscript and insightful discussions. This study was supported by the National Institutes of Health (grants GM-114250 to N.C. and L.M.A. and R01DK041544 to N.C. and G.W.A.).

Author contributions

A.Ll.-E., R.W.M., A.R.-N., G.W.A., L.M.A., and N.C. designed experiments, performed experiments and analyzed and fitted the data. L.M.A. derived the equations. A.Ll.-E., G.W.A., L.M.A. and N.C. wrote the paper.

Competing interests

The authors declare no competing financial interests.

Additional information

Extended data is available for this paper at https://doi.org/10.1038/s41594-020-0417-5.

Supplementary information is available for this paper at https://doi.org/10.1038/s41594-020-0417-5.

Correspondence and requests for materials should be addressed to L.M.A. or N.C.

Peer review information Katarzyna Marcinkiewicz and Ines Chen were the primary editors on this article and managed its editorial process and peer review in collaboration with the rest of the editorial team.

Reprints and permissions information is available at www.nature.com/reprints.

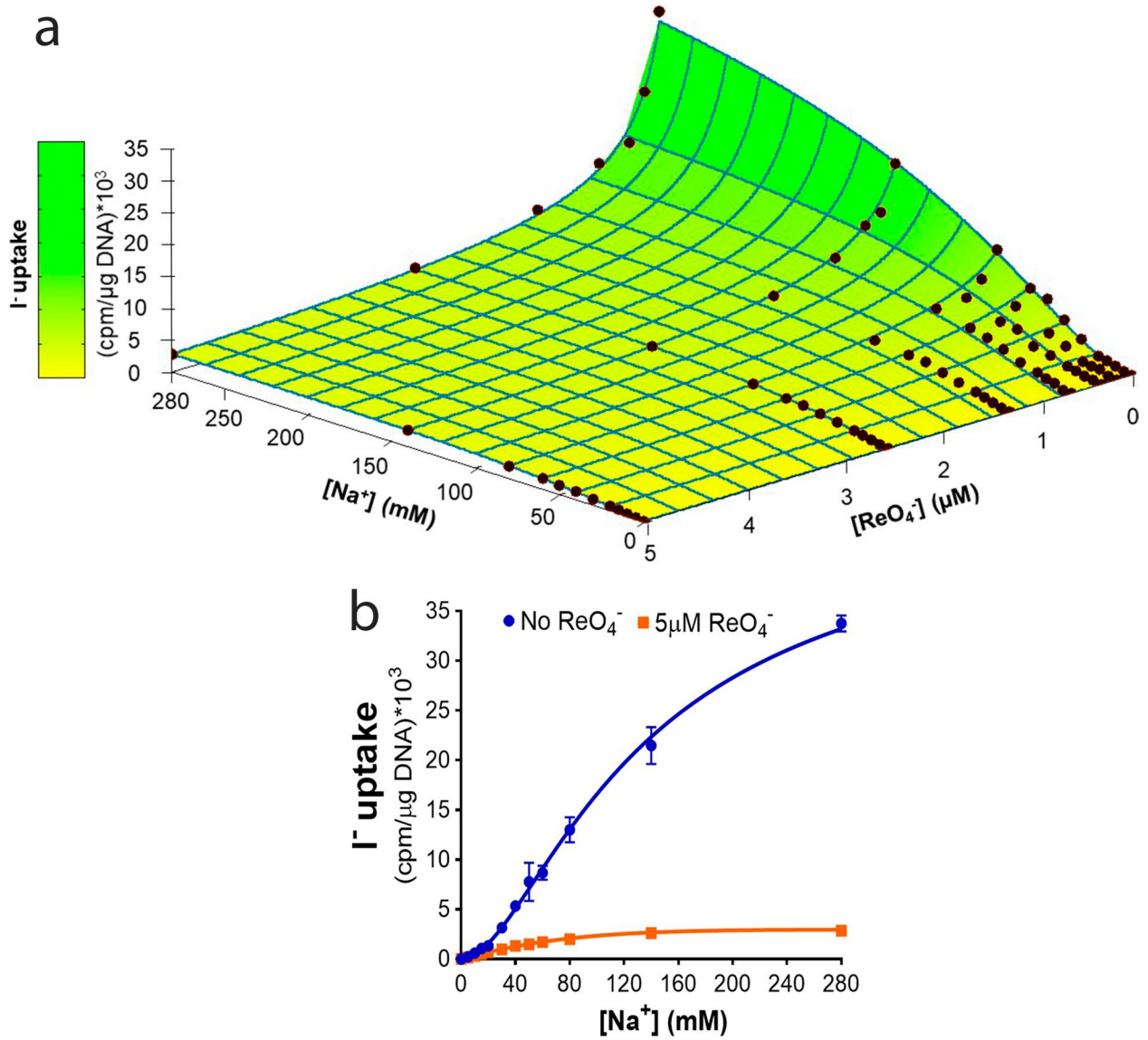

Extended Data Fig. 1 | ReO_4^- changes the stoichiometry of NIS-mediated I^- transport from electrogenic to electroneutral. Initial rates of I^- transport at different concentrations of Na^+ (0-280 mM) and ReO_4^- (0-5µM). Carrier-free $^{125}I^-$ was used as a tracer to determine the effect of ReO_4^- on the mechanism of I^- transport. **a**, Points represent experimental data. The surface, calculated with Equation 3A, represents the rate of transport (cpm/µg DNA), expressed as ν_{max} times the sum of the fraction of NIS species that can transport I^-, that is, the fraction of NIS molecules that are occupied by 2 Na^+ ions and the fraction occupied by 1 Na^+ and ReO_4^- at the NT site.). Points represent the mean of duplicate or triplicate $^{125}I^-$ uptake experiments. **b**, Data from panel a, showing only the experimental points at 0 µM and 5 µM ReO_4^- (that is, the sections of the surface in panel **a** at the concentrations indicated). Points represent the mean of duplicate or triplicate $^{125}I^-$ uptake experiments, error bars represent S.D. Data for all graphs are available as source data.

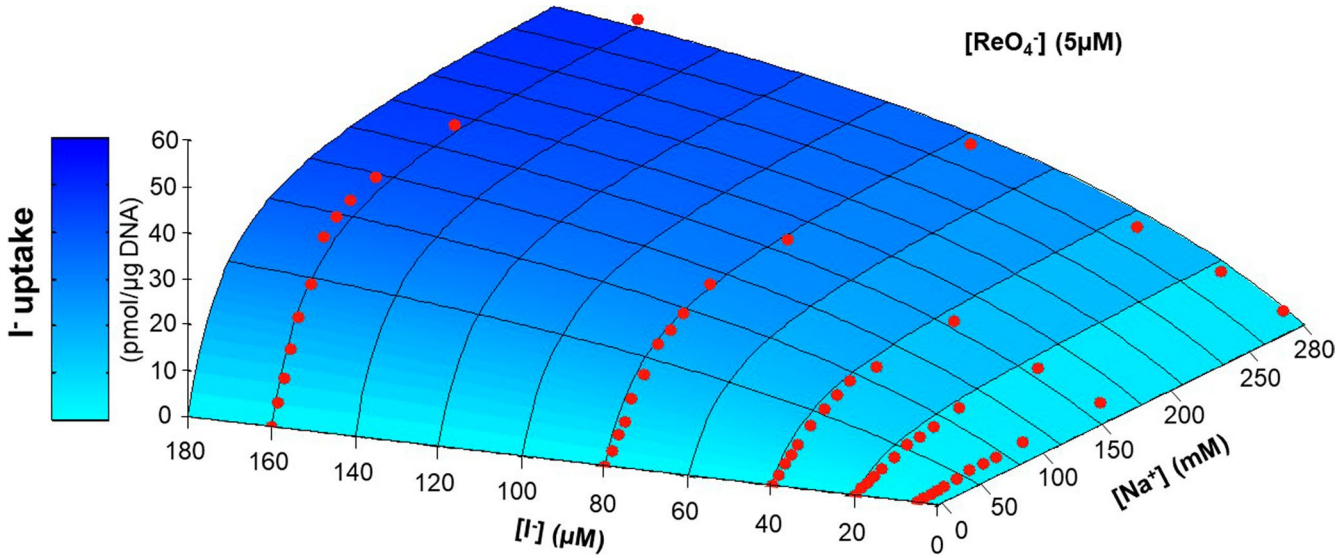

Extended Data Fig. 2 | High concentrations of I^- do not displace ReO_4^- bound to the NT site. Initial rates of I^- transport at different concentrations of I^- (0.75-160 μM), at a constant concentration of ReO_4^- (5 μM), and as a function of the Na^+ concentration (0-280 mM). Data are expressed as pmol of I^-/μg DNA. The surface was calculated using Equation 3B. Points represent the mean of duplicate or triplicate $^{125}I^-$ uptake experiments. Data are available as source data.

nature research

Corresponding author(s): Nancy Carrasco

Last updated by author(s): March 9, 2020

Reporting Summary

Nature Research wishes to improve the reproducibility of the work that we publish. This form provides structure for consistency and transparency in reporting. For further information on Nature Research policies, see Authors & Referees and the Editorial Policy Checklist.

Statistics

For all statistical analyses, confirm that the following items are present in the figure legend, table legend, main text, or Methods section.

n/a	Confirmed	
☐	☒	The exact sample size (*n*) for each experimental group/condition, given as a discrete number and unit of measurement
☐	☒	A statement on whether measurements were taken from distinct samples or whether the same sample was measured repeatedly
☐	☒	The statistical test(s) used AND whether they are one- or two-sided *Only common tests should be described solely by name; describe more complex techniques in the Methods section.*
☒	☐	A description of all covariates tested
☒	☐	A description of any assumptions or corrections, such as tests of normality and adjustment for multiple comparisons
☐	☒	A full description of the statistical parameters including central tendency (e.g. means) or other basic estimates (e.g. regression coefficient) AND variation (e.g. standard deviation) or associated estimates of uncertainty (e.g. confidence intervals)
☒	☐	For null hypothesis testing, the test statistic (e.g. *F*, *t*, *r*) with confidence intervals, effect sizes, degrees of freedom and *P* value noted *Give P values as exact values whenever suitable.*
☒	☐	For Bayesian analysis, information on the choice of priors and Markov chain Monte Carlo settings
☒	☐	For hierarchical and complex designs, identification of the appropriate level for tests and full reporting of outcomes
☒	☐	Estimates of effect sizes (e.g. Cohen's *d*, Pearson's *r*), indicating how they were calculated

Our web collection on statistics for biologists contains articles on many of the points above.

Software and code

Policy information about availability of computer code

Data collection	As described in the manuscript, transport data were collected using a "Cobra quantum 5002 gamma counter." Two-electrode voltage-clamp (TEVC) data were collected using an OC-725C amplifier (Warner Instruments, Hamden, CT) and pClamp10 software (Molecular Devices, Sunnyvale, CA).
Data analysis	As described in the manuscript, we developed statistical thermodynamics equations to analyze transport data. Data were plotted using Gnuplot 5.0 Patchlevel 7. TEVC data were analyzed using Clampfit (Molecular Devices) and Graphpad Prism software (GraphPad, San Diego, CA, USA). The parameters for optimizing the fit of the data to equation 1a or 1b were refined through least squares and manual adjustment with the program Gnuplot 5.0 Patchlevel 7.

For manuscripts utilizing custom algorithms or software that are central to the research but not yet described in published literature, software must be made available to editors/reviewers. We strongly encourage code deposition in a community repository (e.g. GitHub). See the Nature Research guidelines for submitting code & software for further information.

Data

Policy information about availability of data

All manuscripts must include a data availability statement. This statement should provide the following information, where applicable:

- Accession codes, unique identifiers, or web links for publicly available datasets
- A list of figures that have associated raw data
- A description of any restrictions on data availability

Provide your data availability statement here.

Field-specific reporting

Please select the one below that is the best fit for your research. If you are not sure, read the appropriate sections before making your selection.

☒ Life sciences ☐ Behavioural & social sciences ☐ Ecological, evolutionary & environmental sciences

For a reference copy of the document with all sections, see nature.com/documents/nr-reporting-summary-flat.pdf

Life sciences study design

All studies must disclose on these points even when the disclosure is negative.

Sample size	Non-applicable
Data exclusions	None
Replication	456 experimental data points were analyzed through global adjustment of the data. The curves presented in the figures show the mean of duplicates or triplicates for each point value corresponding to each concentration. Transport experiments in mammalian cells were done 2 to 4 times. Two-electrode voltage-clamp (TEVC) measurements in Xenopus laevis oocytes were carried out 8 to 10 times.
Randomization	Non-applicable
Blinding	Non-applicable

Reporting for specific materials, systems and methods

We require information from authors about some types of materials, experimental systems and methods used in many studies. Here, indicate whether each material, system or method listed is relevant to your study. If you are not sure if a list item applies to your research, read the appropriate section before selecting a response.

Materials & experimental systems

n/a	Involved in the study
☒	☐ Antibodies
☐	☒ Eukaryotic cell lines
☒	☐ Palaeontology
☒	☐ Animals and other organisms
☒	☐ Human research participants
☒	☐ Clinical data

Methods

n/a	Involved in the study
☒	☐ ChIP-seq
☒	☐ Flow cytometry
☒	☐ MRI-based neuroimaging

Eukaryotic cell lines

Policy information about cell lines

Cell line source(s)	ATCC
Authentication	Cell lines were not authenticated
Mycoplasma contamination	Cells were not tested for mycoplasma contamination
Commonly misidentified lines (See ICLAC register)	Intestinal embrionic cells (IEC-6). Madin-Darby canine kidney (MDCK) cells